Digital holography as a method for 3D imaging and estimating biovolume of motile cells

Supplementary information

1. Shape from silhouette for QPM

The SFS algorithm is a common method for estimating the 3D shape of an object from its silhouette images. The idea of using silhouettes for 3D shape reconstruction was first introduced in [1], and subsequently different variations of the SFS paradigm have been proposed [2,3]. In [4], optimal positions and directions were derived to take silhouette images for 3D shape reconstruction. Finally, in [5] the authors built a non-invasive 3D digitizer using a turntable and a single camera with SFS as the reconstruction method. The shape estimated using the SFS principle is called Visual Hull (VH) [6], and it has many advantages. In fact, silhouettes are readily and easily obtainable and the implementation of most SFS methods is also relatively straightforward, especially when compared to other shape estimation methods such as multi-baseline stereo [7] or space carving [8]. These advantages have prompted a large number of researchers to apply SFS to solve other computer vision and graphics problems as for example virtual human digitization [9], motion tracking/capture [10,11] and image-based rendering [12]. The silhouette is a binary matrix, obtained by the object image, which contains some information about the 3D shape of the object. In fact, with multiple views of the same object, we can intersect the generalized cones generated by each image to build a volume that contain the object. The limiting smallest volume obtainable in this way is known as the VH of the object. The SFS is attractive because the silhouettes can be computed robustly and quickly using a background subtraction approach. However, the drawback is that even an infinite number of points of view of the object are available, some aspects of the shape are not reported in the final 3D region [13].

For the correct visual hull computation, it is necessary to know the camera model, which can be expressed by the following equation:

$$\mathbf{x} = \mathbf{PX} \tag{1}$$

where $\mathbf{x} = [x, y, 1]^T$ are the image coordinates, $\mathbf{X} = [X, Y, , Z, 1]^T$ are the corresponding 3D point and **P** is a 3x4 matrix called projection matrix or camera matrix. The projection matrix can be factorized in term of intrinsic matrix and extrinsic matrix [13,14]

$$\mathbf{P} = \mathbf{K}[\mathbf{R}\ \mathbf{t}] \tag{2}$$

where **K** is an upper triangular matrix called calibration matrix and describes the camera intrinsically [15]

$$\mathbf{K} = \begin{bmatrix} f_x & s & x_0 \\ 0 & f_y & y_0 \\ 0 & 0 & 1 \end{bmatrix} \tag{3}$$

where f_x and f_y are the focal lengths of the sensor components, s encodes any possible skew between the sensor axes due to the sensor not being mounted perpendicular to the optical axis and $(x_0\ , y_0)$ denotes the optical center expressed in pixel coordinates. [**R t**] is the extrinsic camera matrix where

$$\mathbf{R} = \begin{bmatrix} \cos(\varphi) & \sin(\varphi) & 0 \\ -\sin(\varphi) & \cos(\varphi) & 0 \\ 0 & 0 & 1 \end{bmatrix} \begin{bmatrix} 1 & 0 & 0 \\ 0 & \cos(\theta) & \sin(\theta) \\ 0 & -\sin(\theta) & \cos(\theta) \end{bmatrix} \begin{bmatrix} \cos(\psi) & \sin(\psi) & 0 \\ -\sin(\psi) & \cos(\psi) & 0 \\ 0 & 0 & 1 \end{bmatrix} \tag{4}$$

is the rotation matrix in which $\{\varphi,\theta,\psi\}$ are the Euler angles, and $\mathbf{t} = [t_x\ t_y\ 1]^T$ is the translation vector. In summary, a simple algorithm of SFS consists into the following steps:

1. Recording of several images of the 3D object at different points of view (i.e. different angles).
2. Extraction of the silhouettes by the recorded images.
3. Calculation of the projection matrix for each silhouette.
4. Visual hull computation.

In our experiments on the spermatozoa head's 3D rendering, the steps 1, 2 and 3 are different with respect to the typical case. In fact, the several points of view are obtained through the intrinsic instability of the trapped spermatozoon. For the step 2, we use the algorithm based on the anisotropic diffusion filter, proposed in [15]. Finally, the step 3 consists in computing the angle of the considered point of view for each reconstructed QPM. For this purpose, we compute the best fitted ellipse for the spermatozoon head. Supposing that the rotation occurs around the major axis of the ellipse, the rotation angle is obtained calculating several projected ellipses and comparing them with a tested QPM (see example in Fig.3). Maximizing the SCC between the rotated ellipses and the QPM under consideration, we estimate the angle of the point of view. The estimated angle corresponds to the Euler angles $\{0, \hat{\theta}, 0\}$. Because the rotation of the trapped sperm is limited in the range [0,120] degrees, in order to obtain the silhouettes from other points of view, we complete the silhouettes sequence with the mirror images with respect to the rotation axis.
Finally, the proposed shape algorithm works through the following steps:

1. Recording a sequence of digital holograms of the trapped sperm;
2. Computation of the QPM for each recorded hologram;

3. Extraction of the silhouettes by the QMPs;
4. Computation of the Euler angles for each silhouette;
5. Completing the silhouette sequence with the mirror silhouettes;
6. Calculation of the projection matrix for each silhouette;
7. Visual hull computation.

2. Experimental data

Optical Set-up

A solid state IR laser (3W at 1064nm) is injected into an oil immerse 100x microscope objective (MO, NA=1.3) to obtain a highly focused beam for cell trapping (Fig.1(a)). Another light source, a fiber coupled laser diode (40mW at 660nm), is used for the interferometric measurements. One (collimated) beam passes through the object, the second (reference) beam is recombined to the first thanks to a beam splitter BS. The interference pattern (hologram) is recorded by the CCD2 camera (1280x1024 pixels 5.3µm-sized) positioned at distance "*d*" from the sample image plane, and is then numerically reconstructed for quantitative phase contrast imaging of the sample. All the information for biovolume calculation and 3D rendering are retrieved from the phase mapping of the sperm cell. Another CCD (CCD1) is used to monitor the specimens in the image plane (in focus). The dichroic mirror, DM, ensures the reflection of the IR light and the transmission of the visible laser beam passing thorough the sample (λ=660nm).
Replacing the mirror M with a phase only spatial light modulator (*Holo-Eye PLUTO NIR*), we obtain multiple trapping beams (Fig.1(b)). This latter system consists in an expanded IR light impinging on the liquid crystals display (1cm^2 sized) of the SLM and then reflected into the objective MO, after being opportunely reduced by a system of lenses, not shown here for simplicity. The generated beams are focused by MO into the channel. The geometrical configuration of the focused beams (i.e. the trapping spots) is regulated by a PC: a phase mask named Computer Generated Hologram (CGH) is given as input to the SLM and generate a designed arrangement of the traps in the sample chamber (Fig.1b).

Sample preparation

The bovine sperm cells were prepared by the Institute "Lazzaro Spallanzani" after fixation in suspension of the seminal material with 0.2% glutaraldehyde solution in phosphate buffered saline (PBS) without calcium and magnesium (1:3 v/v). The live ones were kept at -100°C in liquid nitrogen and defrosted for the experiment.

Fabrication of microfluidic channels

The microfluidic channels are fabricated in our labs using Polydimethylsiloxane (PDMS) (Dow Corning SYLGARD 184). In Fig.S1(a) a schematic drawing of the channel is shown. This polymeric channel is obtained moulding the liquid polymer on a "master", with the desired features. Fig.S1(b) shows a bright field image of the double Y shaped microstructure (upper half), with the central channel diameter two times bigger than the others. Thanks to its handiness and flexibility, the PDMS channel could be an ideal tool for rapid prototypization; by using different masters we can

also change the channel dimensions. Moreover, the fluidic micro-channel is reusable, it is sufficient to rinse it out in ultrasounds for few minutes.

A few µL of the sperm solution is injected inside the channel through a little tube; even though we did not use a syringe pump to feed the flux this procedure allowed us to have a continuous flux inside the channel for about one hour. The flux speed has been estimated to be about 50µm/s.

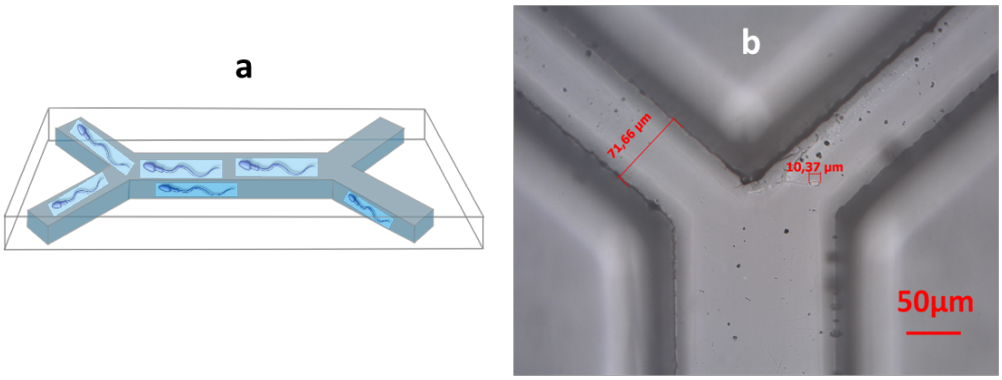

Fig.S1: (a) Drawing of the cells path inside the channel. (b) Microscope image of a spermatozoon inside the micro-channel. The main channel is 150µm width, while the others are 75 µm.

3. Multiple trapping of live spermatozoa

The optical set-up can be improved to perform multiple trapping by HOT configuration [16]. A phase-only SLM (Holo-eye PLUTO NIR) is employed to generate several trapping sites in the microfluidic chamber. Here we perform trapping experiment on several spermatozoa at the same time; in principle we could trap any number of objects, the only limitation being the intensity of each spot (that decreases with increasing the number of spots). In this way it is possible to trap and study in real-time by DHM more cells simultaneously, making a statistical analysis. The use of a microfluidic channel would allow also the selection of the samples, choosing only some of the sperm cells and discarding others [17,18]. In Fig.S2 two sperm cells are trapped simultaneously and analyzed by DHM to obtain the quantitative phase maps of their heads. Then, using the SFS algorithm, it is possible to visualize their 3D shape and calculate the biovolume. Moreover, we are able to manage the relative positions between the trapped cells by refreshing the CGH displayed by the SLM (Fig.S2a-b). The same experiment is also performed on live cells (Fig. S2c and **Supplementary Video 5**), a much more interesting situation for realistic applications.

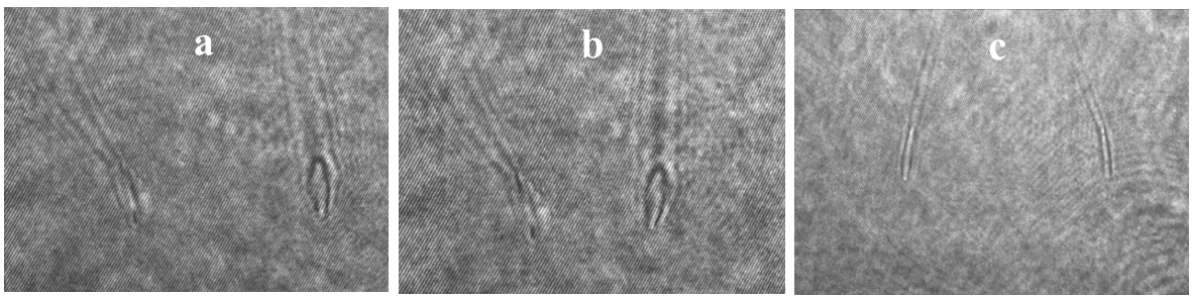

Fig.S2: (a) Two spermatozoa are simultaneously trapped by HOTs. (b) One of them is moved with respect to the other (and rotated in the meantime) by changing the input hologram to the SLM. The cells are out of focus according to the DHM procedure and the interference fringes are well visible. (c) **Supplementary Video 5**: Two live sperm cells are trapped simultaneously. They try to escape the trap, the result being a fast vibration.

References:

1. B. Baumgart, Geometric Modeling for Computer Vision. PhD thesis, Stanford University, 1974.

2. Y. Kim and J. Aggarwal, *IEEE Journal of Robotics and Automation,* 1986, **RA-2**, 127-134.

3. N. Ahuja and J. Veenstra, *IEEE Transactions Pattern Analysis and Machine Intelligence* 1989, **11**, 137-149.

4. K. Shanmukh and A. Pujari, *Pattern Recognition Letter,* 1991, **12**, 165-170.

5. R. Szeliski, *CVGIP: Image Understanding,* 1993, **58**, 23–32.

6. A. Laurentini, *Proc. of the Seventh Scandinavian Conference on Image Analysis*, 1991, 993-1002.

7. M. Okutomi and T. Kanade, *IEEE Transactions on Pattern Analysis and Machine Intelligence,* 1993, **15**, 353-363.

8. K. Kutulakos and S. Seitz, *International Journal of Computer Vision,* 2000, **38**, 199-218.

9. S. Moezzi, L. Tai, P. Gerard, *IEEE Computer Society Multimedia,* 1997, **4**.

10. A. Bottino, A. Laurentini, *Proc. of the Fourth World Multiconference on Systemics*, *Cybernetics and Informatics*, 23-26, 2000.

11. T-W. Su, L. Xue, A. Ozcan, *Proc. Natl. Acad. Sci.*, 2012, **109**, 16018–16022.

12. C. Buehler, W. Matusik, L. McMillan, S. Gortler, Creating and rendering image-based visual hulls, *Technical Report MIT-LCS-TR-780,* 1999.

13. S. Prince, *Computer Vision: models, learning and inference*, Cambridge University Press, 2012.

14. R. Szeliski, *Computer Vision: Algorithms and Applications*, Springer Heidelberg, 2010.

15. P. Memmolo et al., *Opt. Express,* 2011, **19**, 23215-23226.

16. D. Grier, *Nature,* 2003, **424**, 810-816.

17. X. Zhang et al., *Lab Chip,* 2011, **11**, 2535-2540.

18. M. Wang et al., *Nat. Biotech.,* 2005, **23**, 83.